Published in final edited form as:
J Phys Chem B. 2012 June 14; 116(23): 6781–6788. doi:10.1021/jp212399g.

Multilevel X-Pol: A Fragment-based Method with Mixed Quantum Mechanical Representations of Different Fragments

Yingjie Wang[1], **Carlos P. Sosa**[2], **Alessandro Cembran**[1], **Donald G. Truhlar**[1], and **Jiali Gao**[1,2,*]

[1]Department of Chemistry and Supercomputing Institute, University of Minnesota, Minneapolis MN 55455

[2]Biomedical Informatics and Computational Biology, University of Minnesota Rochester, Rochester, MN 55904

Abstract

The explicit polarization (X-Pol) method is a fragment-based quantum mechanical model, in which a macromolecular system in solution is partitioned into monomer fragments. The present study extends the original X-Pol method, where all fragments are treated using the same electronic structure theory, to a multilevel representations, called multilevel X-Pol, in which different electronic structure methods are used to describe different fragments. The multilevel X-Pol method has been implemented into *Gaussian 09*. A key ingredient that is used to couple interfragment electrostatic interactions at different levels of theory is the use of the response density for post-self-consistent-field energy (The response density is also called the generalized density). The method is useful for treating fragments in a small region of the system such as the solute molecules or the substrate and amino acids in the active site of an enzyme with a high-level theory, and the fragments in the rest of the system by a lower-level and computationally more efficient method. The method is illustrated here by applications to hydrogen bonding complexes in which one fragment is treated with the hybrid M06 density functional, Møller-Plesset perturbation theory, or coupled cluster theory, and the other fragments are treated by Hartree-Fock theory or the B3LYP or M06 hybrid density functionals.

Keywords

Mixed fragment method; explicit polarization theory; fragment-based molecular orbital; block-localized density functional theory

1. Introduction

The early development of atomistic potential energy functions[1] for polypeptides and the current coarse-grained models[2] by Scheraga and coworkers have profoundly influenced the field of computational biology. In recent years, a number of fragment-based quantum mechanical methods have been explored.[3–22] In these methods, a large system is partitioned into monomer blocks also called fragments, which may be separate individual molecules or covalently connected species such as amino acid residues in a protein. Fragment-based methods are computationally efficient, which enables electronic structure calculations to be applied to condensed-phase and biomolecular systems to gain a deeper understanding of intermolecular interactions such as polarization and charge transfer.[23–32] Although linear

*gao@jialigao.org, Phone: 612-625-0769, Fax: 612-626-7541.

scaling quantum mechanical calculations of proteins have been carried out,[5,33–36] further approximations are needed to treat intermolecular electrostatic interactions in order to overcome the sampling computational bottleneck for statistical mechanical properties. To this end, the explicit polarization (X-Pol) method, making use of block localization of molecular orbitals within individual fragments,[8,10,37,38] was developed for statistical mechanical Monte Carlo and molecular dynamics simulations of condensed phase[9,39] and biomolecular systems.[40] The block-localization scheme in the X-Pol method can also be applied to density functional theory.[29–30,41–42]

In many applications, one is particularly interested in the properties of a small region of the system, which could be the solute molecule in solution or the active site of an enzyme, and, a high level of theory is needed to yield accurate results for this region of the system. Yet, it is also important to incorporate explicitly the instantaneous polarization of the rest of the system. One approach is to use the method of combined quantum mechanics and molecular mechanics (QM/MM) with the former treating the small region of interest and the latter representing the solvent and protein environment;[43–44] however, most molecular mechanics treatments do not include the mutual polarization effects.[45] Beyond traditional QM/MM approaches, a mixed multilevel fragment-based quantum mechanical method will allow the environmental region also to be modeled by an electronic structure method.[46] The present paper describes such a multilevel method to represent different fragments with different quantum mechanical methods within the X-Pol formalism. The present multilevel X-Pol procedure has been implemented into the *Gaussian 09* program[47] and it is sufficiently general that any theoretical method available in that program can be combined to represent any of the different fragments. Thus, the present approach differs from the strategy in other fragment-based molecular orbital methods to treat different level of theory separately, such as FMO-MP2,[48] FMO-DFT,[49] FMO-coupled cluster,[50] FMO-multiconfiguration,[51] or multilayer with different basis sets;[52] they are all treated in the same footing here. Our method also represents a general strategy for a multilayer QM/QM coupling to study chemical reactions and intermolecular interactions.[18,52–54]

In the following, we first briefly summarize the X-Pol method, which is followed by a discussion of the multilevel X-Pol strategy. The computational details are given in Section 3, and Section 4 presents applications of the multilevel X-Pol method to two hydrogen bonding systems, one involving acetic acid and water and the other being a Zundel ion-water cluster. Section 5 summarizes the main findings of the present study.

2. Theoretical Background

X-Pol theory has a hierarchy of three elements: (1) the construction of the total molecular wave function, (2) the formulation of an effective Hamiltonian, and (3) the reduction of computational costs in electronic integral evaluation.[8–10,38] We first briefly summarize the X-Pol method for the case in which all fragments are treated at the same self-consistent field (SCF) level, and discuss some methods that can be used to include exchange, dispersion and charge transfer contributions. Then, we describe the procedure for a multilevel X-Pol approach with mixed theoretical levels, focusing our attention on post-SCF methods. Throughout this paper, we consider systems that do not have covalent bond connections between different fragments, but the generalization for treating covalently connected fragments can be achieved using methods described previously,[10] in particular by making use of the generalized hybrid orbital (GHO) scheme developed for combined QM/MM simulations at various levels of theory.[55–59]

2.1. The X-Pol Method

In X-Pol, a macromolecular system is partitioned into N monomer blocks, also called fragments, and the total wave function Ψ of the system is written as a Hartree product of the antisymmetric wave functions of individual fragments:[8]

$$\Psi=\prod_{A=1}^{N}\Psi_A \tag{1}$$

where Ψ_A is the wave function of fragment A, which may be approximated by a single determinant or by a multi-configurational wave function. The wave functions for different monomers do not have to be approximated using the same method or represented at the same level of theory.

The effective X-Pol Hamiltonian for the system is

$$\hat{H}=\sum_{A}^{N}\hat{H}_A^o+\frac{1}{2}\sum_{A}^{N}\sum_{B\neq A}^{N}(\hat{H}_{AB}^{\text{int}}+E_{AB}^{\text{XD}}) \tag{2}$$

where $\hat{H}_A^o$ is the electronic Hamiltonian for an isolated fragment A, and $\hat{H}_{AB}^{\text{int}}$ and E_{AB}^{XD} represent electrostatic and exchange-dispersion (XD) interactions between fragments A and B.[8,10,38] The interaction Hamiltonian $\hat{H}_{AB}^{\text{int}}$ depends on both electronic and nuclear degrees of freedom, and it can be viewed as an electrostatic embedding of the QM fragment A in the external field of fragment B:

$$\hat{H}_{AB}^{\text{int}}=-\sum_{i=1}^{M_A}e\,\Phi_{\text{E}}^{B}(\mathbf{r}_i^A)+\sum_{\alpha=1}^{N_A}Z_\alpha^A\Phi_{\text{E}}^{B}(\mathbf{R}_\alpha^A) \tag{3}$$

where M_A and N_A are, respectively, the number of electrons and nuclei of fragment A, $\mathbf{r}_i^A$ and $\mathbf{R}_\alpha^A$ are the corresponding positions for electron i and nucleus α, Z_α^A is a nuclear charge, and $\Phi_{\text{E}}^{B}(\mathbf{r}_x^A)$ is the electrostatic potential at $\mathbf{r}_x^A$ due to the external charge density of fragment B:

$$\Phi_{\text{E}}^{B}(\mathbf{r}_x^A)=\int\frac{\rho^B(\mathbf{r}')}{|\mathbf{r}_x^A-\mathbf{r}'|}d\mathbf{r}' \tag{4}$$

where $\rho^B(\mathbf{r}')=-\rho_{ele}^B(\mathbf{r}')+\sum_b Z_b^B\delta(\mathbf{r}'-\mathbf{R}_b^B)$ is the total charge density of fragment B, including both the smooth electron density $\rho_{ele}^B(\mathbf{r}')$ and the nuclear charges $\{Z_b^B\}$ at $\{\mathbf{R}_b^B\}$. In the present multilevel X-Pol, the embedding potential $\Phi_{\text{E}}^{B}(\mathbf{r}_x^A)$ is modeled by partial atomic charges $\{q_b^B[\rho_{ele}^B]\}$ derived from the corresponding charge density, ρ_{ele}^B, for example by population analysis (Mulliken or Löwdin charges) or by electrostatic potential fitting (CHELPG or Merz-Kollman schemes), and this simplifies it to

$$\Phi_{\text{E}}^{B}(\mathbf{r}_x^A)=\sum_b\frac{q_b^B}{|\mathbf{r}_x^A-\mathbf{R}_b^B|} \tag{5}$$

The theory can be extended to use higher multipole moments[60] or even the full charge distribution of the fragments (eq 4) to compute the electrostatic potential,[61] but that will not be considered here.

The total X-Pol energy is given as follows:

$$E[\{\rho\}]=<\Psi\,|\,\mathrm{H}\,|\,\Psi>=\sum_{A}^{N}E_{A}+\frac{1}{2}\sum_{A}^{N}\sum_{B\neq A}^{N}E_{AB}^{\mathrm{int}}[\rho^{A},\{q_{b}^{B}\}]+E_{AB}^{\mathrm{XD}} \tag{6}$$

where E_A is the energy of fragment A (note that E_A is different from the gas-phase energy E_A^o because the wave function Ψ_A has been polarized by the rest of the system in X-Pol), and $E_{AB}^{\mathrm{int}}[\rho^A,\{q_b^B\}]$ is the electrostatic interaction energy between fragments A and B, akin to that used in a QM/MM method.[43–44]

The energy term E_{AB}^{XD} in eq 4 accounts for the effects of the approximation used in eq 1, which by construction neglects short-range exchange repulsion and long-range dispersion interactions as well as charge transfer contributions. In the original X-Pol method,[8,10] exchange repulsion is represented by a pairwise R_{IJ}^{-12} dependence and the attractive non-covalent interaction by a pairwise R_{IJ}^{-6} term as in the Lennard-Jones potential, where R_{IJ} is an interatomic distance. In the present study, an exponential function for the repulsion, as in the Buckingham potential is used:

$$E_{AB}^{\mathrm{XD}}=\sum_{I}^{N_A}\sum_{J}^{N_B}A_{IJ}e^{-B_{IJ}\cdot R_{IJ}}-\frac{C_{IJ}}{R_{IJ}} \tag{7}$$

where the parameters A_{IJ}, A_{IJ}, and C_{IJ} are determined using standard combining rules from atomic parameters such that $A_{IJ}=(A_IA_J)^{1/2}$, $B_{IJ}=(B_I+B_J)/2$, and $C_{IJ}=(C_IC_J)^{1/2}$.

The effect of charge transfer is modeled indirectly. The strict block localization of molecular orbitals within individual monomers in X-Pol does not allow charge delocalization between different fragments (unless one uses a grand canonical formulation, which is not employed here).[31] At distances longer than hydrogen bonding range, it is often a good approximation to neglect charge transfer, and interfragment electrostatic interactions can then be adequately described by the electrostatic embedding scheme[43–44] using the Coulomb potential (eq 5). However, at short interfragment distances where there is significant orbital overlap, one needs to take into account the energy component due to charge delocalization (sometimes also called charge transfer).[30–31,61] In the present work, we account for charge transfer only empirically, in particular (in the spirit often used in molecular mechanics)[62] by modeling the charge delocalization energy with enhanced electrostatic polarization. Consequently, the electrostatic potential $\Phi_{\mathrm{E}}^{B}(\mathbf{r}_x^A)$ in eq 5 is recognized as an effective potential that mimics both long-range Coulomb (electrostatic) interactions and short-range charge delocalization contributions, and this can be achieved to some extent by optimizing the parameters in the E_{AB}^{XD} term (eq 7) and possibly the charge model[63] $\{q_b^B[\rho_{ele}^B]\}$ (eq 5) to best reproduce hydrogen bonding interactions for a set of bimolecular complexes[38] (however such optimization is beyond the scope of the present article).

Beyond the empirical approximations, a variational many-body expansion approach in X-Pol has been described, which includes exchange repulsion, charge delocalization and dispersion terms explicitly.[64] Individually, one way to improve on the repulsive potential is to antisymmetrize the X-Pol Hartree-product wave function;[61,65–68] this yields X-Pol with full eXchange, called X-Pol-X.[69] When the monomers are treated by Hartree-Fock theory, this calculation can be accomplished by using the formalisms of block-localized wave function (BLW)[61,67–68] or the SCF-MI method,[65] and this procedure has been extended to density functional theory.[29–30,42] To treat dispersion interactions, multiconfigurational

methods and perturbation theories can be used; for example, one can adopt symmetry adapted perturbation theory (SAPT) as a post-SCF correction to the X-Pol energy,[70] as has been done recently by Jacobson and Herbert.[22] Both exchange-repulsion and dispersion interactions are of short range on the length scale of solutions and biopolymer systems, and only the close neighbors need to be explicitly considered.[69]

Charge delocalization effects can also be estimated using a grand canonical ensemble,[31] or by using the method of interaction energy expansion introduced by Stoll and Preuss,[71] which has been adopted by Kitaura and coworkers in a fragment molecular orbital implementation.[11] Of course, a straightforward way of including charge delocalization effects is to use larger fragments that include charge transfer partners.[28] Another approach, which has been recast in several ways, is the molecular fractionation with conjugated caps (MFCC) approach by Zhang and coworkers.[13,72] In MFCC, the individual fragments are capped with a structure representative of the local functional group of the original system, and the total energy is obtained by subtracting the energies that account for the common fragments used in the "caps".[73–74] In both cases, the total energy can be conveniently determined using this addition-subtraction scheme; however, the total molecular wave function is no longer available, making energy gradient calculations more challenging. In this regard, we have developed a generalized explicit polarization (GX-Pol) method on the basis of a multiconfiguration self-consistent field (MCSCF) wave function that makes use of dimeric, charge-delocalized fragments.[30,75] In the present study, we do not include the explicit treatment of charge delocalization energy, but this can be addressed in a separate study.

2.2. Multilevel X-Pol

The method outlined in the previous section has been implemented with all fragments treated at the same theoretical level (semiempirical,[8,10,37] Hartree-Fock (HF), or density functional theory (DFT)[38]). Here, we consider a system partitioned into N fragments, of which N' fragments are treated by a method denoted as high level (HL) and the remainder $N - N'$ fragments are modeled with a different approach specified as low level (LL). The former fragments are called HL fragments, and the latter are called LL fragments. Generalization to any number of levels is straightforward, but for convenience, we restrict the following discussions to two levels. This division highlights the need for high accuracy in a small (HL) region of interest, such as the solute molecule in a solution or the active site of an enzyme, while retaining the need for a computationally efficient way to include polarization effects in the remainder of the system. In the present illustration of the method, the LL method is restricted to either HF or DFT.

A variety of methods can be used for fragments in the HL region, and they are divided into two categories: SCF and post-SCF. For methods such as DFT and multiconfiguration SCF (MCSCF), the treatment is the same as described previously[38] for single-level X-Pol based on ab initio Hartree-Fock calculations or DFT. The second category includes post-SCF methods such as configuration interaction (CI), coupled cluster (CC) and Møller-Plesset (MP) perturbation theory; when such methods are employed for HL fragments, the total X-Pol energy is written as

$$E[\{\rho\}]=\sum_{A}^{N}\left(E_{A}^{\mathrm{SCF}}+\frac{1}{2}\sum_{B\neq A}^{N}E_{AB}^{\mathrm{int}}[\rho^{A},\{q_{b}^{B}\}]+E_{AB}^{\mathrm{XD}}\right)+\sum_{A}^{N'}E_{\mathrm{A}}^{\mathrm{corr}}=E_{\mathrm{tot}}^{\mathrm{SCF}}+E_{\mathrm{tot}}^{\mathrm{corr}} \quad (8)$$

where E_{A}^{SCF} is the SCF energy of the reference wave function, E_{A}^{corr} is the post-SCF correction for fragment A, and $E_{\mathrm{tot}}^{\mathrm{SCF}}$ and $E_{\mathrm{tot}}^{\mathrm{corr}}$ are the total SCF energy and the total post-

SCF correlation energy. Note that the SCF energy E_A^{SCF} can be obtained either from a single determinant reference wave function in a CI, CC, or MP2 calculation or a multiconfiguration wave function in multireference CI, or CASPT2, etc. calculations. The main difference of this energy expression from that of eq 6 is that the total multilevel X-Pol energy is no longer written as the expectation value of an X-Pol wave function.

In using eq 8, the computation involves an initial optimization of the X-Pol SCF wave function, followed by determining the post-SCF energy corrections for fragments in the HL region. In the SCF procedure, the charge densities of the HL fragments that polarize other fragments are the response densities corresponding to the post-SCF calculation.[76–78] The response density (which is also called the generalized density and relaxed density) is the sum of the SCF density and the relaxation density due to the post-SCF procedure, which is obtained using the Z-vector method,[79] including a single coupled perturbed HF calculation for the occupied and virtual molecular orbital (MO) block, independent of the specific post-SCF method.[77] The response density procedure allows the use of methods (such as MP perturbation theory) for which the energy does not correspond to a wave function expectation value; it is also more accurate for computing one-particle properties using CC and other post-SCF methods. The response density is obtained by adding the relaxation density to the SCF density and transforming into the atomic basis for population analysis and computation of one-particle properties including the electrostatic potential:

$$P_{\mu\nu}^{A,\mathrm{HL}}=P_{\mu\nu}^{A,\mathrm{SCF}}+P_{\mu\nu}^{A,\mathrm{rel}} \tag{9}$$

where $P_{\mu\nu}^{A,\mathrm{SCF}}$ and $P_{\mu\nu}^{A,\mathrm{rel}}$ are the SCF and relaxation densities for fragment A in the HL region. If Mulliken population analysis (MPA) is used,[80] the partial atomic charges in eq 8 for HL fragments can be written as

$$q_a^{A,\mathrm{HL}}=Z_a^A-\sum_{\substack{\mu\in a\\ \nu}}P_{\mu\nu}^{A,\mathrm{HL}}S_{\mu\nu}^A=q_a^{A,\mathrm{SCF}}+q_a^{A,\mathrm{rel}} \tag{10}$$

The elements of the effective Hamiltonians (Fock or Kohn-Sham matrices), both for the HL and LL fragments, in a multilevel X-Pol method can be written similarly as[22,81]

$$\mathbf{F}_{\mu\nu}^{A,\mathrm{Xpol}}=\frac{\partial E^{\mathrm{SCF}}[\{\rho\}]}{\partial P_{\mu\nu}^{A,\mathrm{SCF}}}=\mathbf{F}_{\mu\nu}^{A,o}-\frac{1}{2}\sum_{B\neq A}\sum_{b\in B}q_b^B\left(\mathbf{I}_b^B\right)_{\mu\nu}^A+\frac{1}{2}\sum_{a\in A}X_a^A\left(\mathbf{\Lambda}_a^A\right)_{\mu\nu} \tag{11}$$

where $\mathbf{F}_{\mu\nu}^{A,o}$ the Fock matrix element for an isolated fragment A, q_b^B is the partial charge on atom b in fragment B and it is understood that $q_b^B\equiv q_b^{B,\mathrm{HL}}$ for fragments in the HL region, $\mathbf{I}_b^B$ is the matrix of the pair potential in atomic basis as defined by

$$\left(\mathbf{I}_b^B\right)_{\mu\nu}^A=\langle\mu|\frac{1}{|\mathbf{r}-\mathbf{R}_b^B|}|\nu\rangle \tag{12}$$

and X_a^A is a vector arising from the derivative of the interaction energy with respect to partial atomic charge of atom a:

$$X_a^A=\sum_{B\neq A}\left(\sum_{\lambda\sigma}P_{\lambda\sigma}^B\left(\mathbf{I}_a^A\right)_{\lambda\sigma}^B+\sum_{b\in B}\frac{Z_b^B}{|\mathbf{R}_b^B-\mathbf{R}_a^A}\right) \tag{13}$$

Note that the notation $P^B_{\lambda\sigma}$ is defined as $P^B_{\lambda\sigma} \equiv P^{B,\mathrm{HL}}_{\lambda\sigma}$ if $B \leq N$', and as $P^B_{\lambda\sigma} \equiv P^{B,\mathrm{SCF}}_{\lambda\sigma}$ if $B>N$'. The elements of the response density matrix, $\mathbf{\Lambda}^A$, are given by

$$\left(\mathbf{\Lambda}^A_a\right)_{\mu\nu} = \frac{\partial q^A_a}{\partial P^{A,\mathrm{SCF}}_{\mu\nu}} = \frac{\partial q^{A,\mathrm{SCF}}_a}{\partial P^{A,\mathrm{SCF}}_{\mu\nu}} \tag{14}$$

where q^A_a is the atomic charge on atom a, and $P^{A,\mathrm{SCF}}_{\mu\nu}$ is an element of the density matrix of fragment A in the SCF optimization of the X-Pol fragment wave function. The charge derivatives have been given for a number of charge models.[22,81] The interpretation of eqs 11–14 is that the wave functions for all fragments are optimized at the SCF level, but their polarization, by virtue of setting q^B_b to $q^{B,\mathrm{SCF}}_b + q^{B,\mathrm{rel}}_b$ for $B \leq N$', includes contributions from the relaxation density corresponding to the post-SCF energy in the HL region.

2.3. Iterative Updating (IU) Method

In the standard X-Pol method, the SCF wave function of eq 1 is optimized variationally by using eq 11.[81] An alternative way of optimizing the SCF wave function, which is non-variational, is to consider each fragment as an isolated molecule embedded in the electrostatic field of the rest of the system. Then, the Fock matrix for each fragment can be written separately as follows:[8–10]

$$\mathbf{F}^{A,\mathrm{IU}} = \mathbf{F}^{A,o} - \sum_{B\neq A}\sum_{b\in B} q^B_b \left(\mathbf{I}^B_b\right)^A \tag{15}$$

where $\mathbf{F}^{A,o}$ is the Fock matrix of fragment A, $\mathbf{q}^B_b$ is a column vector of atomic charges of fragment B stretched to the dimension of the orbital basis and $\left(\mathbf{I}^B_b\right)^A$ is the matrix of pair potential (eq 12). The total electronic energy of the system can then be determined iteratively by a double self-consistent-field (DSCF) procedure.[8–10,82] Starting with an initial guess of the one-electron density matrix for each fragment, one loops over all fragments in the system and performs SCF optimization of the wave function for each fragment in the presence of the instantaneous external charges of all other fragments (through $\left(\mathbf{I}^B_b\right)^A$). This is iterated (the SCF for the system) with an updated external potential until the total electronic energy and the charge density are converged. This iterative updating (IU) procedure is straightforward and was the approach proposed for fragment calculations in Ref. 8 and adopted in the subsequent FMO implementation.[11,83] Such an iterative updating procedure can be found in many applications both in electronic structure theory[82] and combined QM/MM approaches that include MM polarization.[45] A main short coming of the above approach is that the Fock matrix in eq 15 is not variationally optimized,[18,81] and it is not suitable for efficiently computing energy gradients. In this study, we use the superscript IU for the non-variational iterative updating procedure in eq 15, and simply Xpol for the variational method employing eq 11.

Note that both the sequential and variational optimization of the X-Pol wave function can be carried out by DSCF iterations, although they can also be done, if desired, as a single large SCF problem. In the illustrations of the multilevel X-Pol method presented below, we will we compare the energy difference between the two optimization procedures.

3. Computational details

The goal of this study is to illustrate that the multilevel X-Pol fragment-based quantum mechanical model can be implemented with an arbitrary combination of different electronic

structural methods for different fragments. The X-Pol method has been implemented into a locally modified version of the *Gaussian-09* program.[47] In this program, the response density[78] can be computed for a range of post-SCF methods, including MPn, QCISD, CCD, CCSD, CID, CISD, BD, and SAC-CI,[47] thus, any of these—as well as SCF methods—can be used to represent a given fragment in multilevel X-Pol.

We choose two hydrogen bonding complexes, (1) acetic acid (fragment *A*) and water (fragment *B*), and (2) $H_5O_2^+$ (fragment *A*) and four water molecules (four water fragments as *B* for a total of five fragments). The complexes and monomer structures are optimized using the hybrid M06/MG3S DFT, which are then used in all subsequent single-point energy calculations with various multilevel X-Pol methods. In the present study, we have used the hybrid density functional theory M06, second order Møller-Plesset perturbation theory (MP2), and coupled-cluster with singles and doubles (CCSD) method for acetic acid and the $H_5O_2^+$ ion, and we employed Hartree-Fock (HF), B3LYP[84] and M06[85] density functional method for water. In all X-Pol calculations, the 6-31G(d) basis set was used.

The binding energy ΔE_b for the complex is defined as

$$\Delta E_b = E_{AB} - E_A^o - E_B^o \tag{16}$$

In X-Pol, the binding energy can be decomposed into an intramolecular distortion term ΔE_{dist}, including both the energy change due to geometric variation and the energy cost needed to polarize the electron density, and an intermolecular interaction contribution.[30,43,61] The latter can be further separated into an electrostatic component ΔE_{int} and an exchange-dispersion energy term ΔE_{XD}. In this energy decomposition scheme, we rewrite eq 16 as

$$\Delta E_b = \Delta E_{\text{dist}} + \Delta E_{\text{int}} + \Delta E_{\text{XD}} \tag{17}$$

These terms are defined as follows:

$$\Delta E_{\text{dist}} = \sum_A^N (E_A - E_A^o) \tag{18}$$

where E_A and E_A^o are the intra-monomer components of the energies of monomer *A* in the complex or in isolation,

$$\Delta E_{\text{XD}} = \sum_{A>B}^N E_{AB}^{\text{XD}} \tag{19}$$

and

$$\Delta E_{\text{int}} = \sum_{A>B}^N \Delta E_{AB}^{\text{int}} = \sum_{A>B}^N \frac{1}{2}[\Delta E_A^{\text{int}}(B) + \Delta E_B^{\text{int}}(A)] \tag{20}$$

where $\Delta E_{AB}^{\text{int}}$ is the interaction energy between monomers *A* and *B*, and $\Delta E_X^{\text{int}}(Y)$ is the electrostatic interaction energy of the "QM" fragment *X* polarized by the external potential of monomer *Y*. Although $\Delta E_X^{\text{int}}(Y)$ and $\Delta E_Y^{\text{int}}(X)$ describe the same interaction between monomers *X* and *Y*, they are not symmetric unless the same theoretical model is used for both monomers and the Coulomb integrals are explicitly computed over all basis functions.

For convenience of discussion, we also define the total electrostatic component of binding energy as

$$\Delta E_{\text{ele}} = \Delta E_{\text{dist}} + \Delta E_{\text{int}} \quad (21)$$

4. Results and discussion

Tables 1 shows the computed electrostatic interaction energies between acetic acid and water for the optimized configuration shown in Figure 1 using the sequential optimization approach in multilevel X-Pol. Two charge models are used in this work, those from Mulliken population analysis (MPA) and those from Merz-Kollman electrostatic potential fitting (MK). The corresponding results obtained using variational optimization in multilevel X-Pol are given in Table 2. In this case, only the MPA charges are used.

The total interaction energy between an acetic acid and a water molecule at the configuration shown in Figure 1 is −6.9 kcal/mol from M06/MG3S optimization, which is reduced slightly to −6.6 kcal/mol using CCSD(T)/MG3S//M06/MG3S. The electrostatic interaction energy from X-Pol by iterative updating method using M06/6-31G(d) for both fragments is −7.7 kcal/mol when the MPA charges are used, and it is reduced to −7.0 kcal/mol when the MK charges are used. With a different combination in the multilevel X-Pol method in which acetic acid is treated by CCSD(T) and water by M06, the computed electrostatic interaction energies are −7.6 and −7.2 kcal/mol with the MPA and MK charges, respectively, similar to the single level results. Switching to the variational X-Pol method, we obtained an electrostatic interaction energy of −9.0 kcal/mol using the M06 representation of both monomers and the MPA charges. In this case, the variational optimization of the Kohn-Sham orbitals lowers the energy by 1.8 kcal/mol for this bimolecular complex. Similar trends are found in other multilevel X-Pol combinations in Table 2. The results in Table 1 do not include the exchange repulsion energy, charge transfer contributions, or correlation effects that result from wave function delocalization in a full KS-DFT calculation. The latter two effects are not fully separable in energy decomposition analyses, but both make stabilizing contributions to the bimolecular complex, which tend to partially compensate the strong exchange repulsion energies. If we optimize the empirical parameters in eq 7 for the M06 and B3LYP combination in multilevel X-Pol, we obtained a energy of of 2.1 kcal/mol for the ΔE_{XD} term, which is applied to all multilevel X-Pol methods in Table 2 to yield the total binding energies ΔE_b.

Table 1 shows that the MPA charges tend to provide stronger electrostatic polarization effect than do the MK charges. This results in overall interaction energies that are greater in magnitude. Both $\Delta E_A^{\text{int}}(B)$ and $\Delta E_B^{\text{int}}(A)$ describe the electrostatic interaction energy between fragments A and B, but they differ numerically because the former specifies embedding of fragment A in the classical field of fragment B whereas $\Delta E_B^{\text{int}}(A)$ gives the embedding energy of fragment B in the electrostatic field of fragment A. Across the series of five different combinations shown in Tables 1, the computed $\Delta E_A^{\text{int}}(B)$ values are greater than the $\Delta E_B^{\text{int}}(A)$ terms by using IU optimization of the wave function within an electrostatic embedding picture; however, the ordering is reversed in the variational X-Pol method. Furthermore, the electrostatic polarization is significantly stronger by variational optimization than by IU optimization of the wave function, both in single level and in multilevel X-Pol. On one hand, the difference between the $\Delta E_A^{\text{int}}(B)$ and $\Delta E_B^{\text{int}}(A)$ terms highlights the asymmetry in the representation of two fragments in a QM/MM type of treatment, and the average of the two terms is defined as the X-Pol dimer interaction energy (eq 20).[8–9] On the other hand, the difference between the IU and variational optimization

procedures for the X-Pol wave function shows the importance of correctly accounting for the mutual polarization effects among different fragments that minimize the adiabatic ground state energy. Note that few existing fragment-based methods optimize the fragment wave functions variationally.

Table 3 gives the interaction energies between the Zundel ion $H_5O_2^+$ and four water molecules computed with various theoretical models using the optimized structure with M06/MG3S[86] (Figure 2). The optimized structure for the complex is very similar to that optimized using B3LYP/6-311+G(dp) from ref 87.

It is interesting to first compare various methods of estimating the exchange repulsion–dispersion contributions to the energy of binding in this case. The exchange repulsion energy can be obtained as the difference between the energy from the antisymmetrized X-Pol wave function and that from the X-Pol at the Hartree-Fock level. We found that the results depend noticeably on the basis set and the charge model used for electrostatic coupling between different fragments (eq 11). The estimated exchange energies are 30.0 and 28.5 kcal/mol using iterative updating optimization in X-Pol with the MK and MPA charges, respectively. This increases to 35.8 kcal/mol using the variational X-Pol wave function and the MPA charges. In these cases, the 6-31G(d) basis is used.

To gain more insights into the magnitude of the contributions from inter-monomer exchange, dispersion and charge transfer on the hydrogen bonding interactions in the Zundel ion complex, we have carried out an interaction energy decomposition analysis using the block-localized wave function method (BLW-ED) using a larger basis set.[30,61] At the HF/aug-cc-pVDZ level, the exchange repulsion and charge transfer contributions to the energy of binding are estimated to be 38.8 and −13.3 kcal/mol, respectively, for a net contribution of 25.5 kcal/mol, and the total binding energy is −62.4 kcal/mol. If one uses the difference between the CCSD(T) binding energy (−69.7 kcal/mol) and that at the HF level (−62.4 kcal/mol) as a rough estimate of the dispersion contribution, a value of −7.3 kcal/mol is obtained. Then, the overall E_{AB}^{XD} term including the effect of charge transfer may be estimated as 18.2 kcal/mol (that is, 25.5 minus 7.3 kcal/mol).

We optimized the Lennard-Jones parameters separately for the oxonium ion system with the M06 density functional for $H_5O_2^+$ and the B3LYP functional for $(H_2O)_4$, and we obtained $A_{OO} = 1.5221\times10^5$ kcal/mol, $B_{OO} = 3.754$ Å, and $C_{OO} = 756.3$ Å^6 kcal/mol for the Buckingham potential (eq 7). Then, eq 7 yields a value of 18.4 kcal/mol for ΔE_{XD}, in good agreement with the above analysis. Although the ΔE_{XD} term ought be reoptimized for each multilevel X-Pol model, we have used to same Buckingham energy for all combinations listed in Table 3, and the total binding energies in the last column of Table 3 are reasonable in comparison with the CCSD(T) value (at the M06/MG3S geometry) of −69.7 kcal/mol. For comparison, the corresponding multilevel X-Pol values without inclusion of the ΔE_{XD} term are significant greater than the full QM result, ranging from −83 to −92 kcal/mol.

For multilevel X-Pol in which both HL and LL energies are obtained at the SCF level, the energy of binding from the variational approach will be more negative than that obtained using the non-variational (iterative updating) procedure, which is also used in the fragment molecular orbital model.[11–12] The results using the M06 density functional for the HL fragment in Table 3 are indeed consistent with this expectation. However, if the HL energy is determined by a post-SCF theory as in MP2 and CCSD calculations in Table 3, there is no guarantee that the “variational” multilevel X-Pol energy is lower than that of the IU optimization result because only the reference wave function used in the post-SCF calculation is optimized. This is seen in the CCSD and M06 combination, which yields a binding energy smaller than that from the IU optimization method (both using the MPA

charges). The reference wave functions for the individual fragments are more strongly distorted than in other cases.

5. Concluding remarks

The explicit polarization (X-Pol) method is a fragment-based quantum mechanical method, in which a macromolecular system is partitioned into monomer fragments and the total molecular wave function is written as a Hartree product of the antisymmetric wave functions for individual fragments. In the present study, a general formulation is presented to treat different fragments with different electronic structure methods. The current implementation of the multilevel X-Pol method in *Gaussian-09* allows any method available in that program to be used to describe a given fragment. The key to the implementation is using the response density to compute the electrostatic coupling (and mutual polarization), in particular by using the response density in population analyses or in an electrostatic potential charge fitting procedure.

The computational method is illustrated by calculations on two hydrogen bonding complexes involving acetic acid and water, and the $H_5O_2^+$ ion and four water molecules. Acetic acid and $H_5O_2^+$ are treated using M06, MP2 and CCSD as the high-level theory, and these methods are paired with one of HF, M06 and B3LYP as the lower-level method. The present multilevel X-Pol method can be used to treat a small region of the system, such as the solute molecule in solution or the active site of an enzyme, with a high-level theory, and the remainder of the system with a more computationally efficient method.

Acknowledgments

This work was supported in part by the National Science Foundation under award nos. CHE09-57162 and CHE09-56776 and the National Institutes of Health under award nos. GM46376 and GM091445. All computations were carried out at the Minnesota Supercomputing Institute.

References

1. Momany FA, Mcguire RF, Burgess AW, Scheraga HA. J. Phys. Chem. 1975; 79:2361.
2. Liwo A, Oldziej S, Czaplewski C, Kleinerman DS, Blood P, Scheraga HA. J. Chem. Theory Comput. 2010; 6:890. [PubMed: 20305729]
3. Gordon MS, Fedorov DG, Pruitt SR, Slipchenko LV. Chem. Rev. 2012; 112:632. [PubMed: 21866983]
4. Yang W. Phys. Rev. Lett. 1991; 66:1438. [PubMed: 10043209]
5. Stewart JJP. Int. J. Quantum Chem. 1996; 58:133.
6. Dixon SL, Merz KM Jr. J. Chem. Phys. 1996; 104:6643.
7. Dixon SL, Merz KM Jr. J. Chem. Phys. 1997; 107:879.
8. Gao J. J. Phys. Chem. B. 1997; 101:657.
9. Gao J. J. Chem. Phys. 1998; 109:2346.
10. Xie W, Gao J. J. Chem. Theory Comput. 2007; 3:1890. [PubMed: 18985172]
11. Kitaura K, Ikeo E, Asada T, Nakano T, Uebayasi M. Chem. Phys. Lett. 1999; 313:701.
12. Fedorov DG, Kitaura K. J. Phys. Chem. A. 2007; 111:6904. [PubMed: 17511437]
13. Zhang DW, Xiang Y, Zhang JZH. J. Phys. Chem. B. 2003; 107:12039.
14. Dahlke EE, Truhlar DG. J. Chem.Theory Comput. 2007; 3:46.
15. Dahlke EE, Truhlar DG. J. Chem. Theory Comput. 2007; 3:1342.
16. Tempkin JOB, Leverentz HR, Wang B, Truhlar DG. J. Phys. Chem. Lett. 2011; 2:2141.
17. Dulak M, Kaminski JW, Wesolowski TA. J. Chem. Theory Comput. 2007; 3:735.
18. Hratchian HP, Parandekar PV, Raghavachari K, Frisch MJ, Vreven T. J. Chem. Phys. 2008; 128 034107/1.

19. Mayhall NJ, Raghavachari K. J. Chem. Theory Comput. 2011; 7:1336.
20. Reinhardt P, Piquemal J-P, Savin A. J. Chem. Theory Comput. 2008; 4:2020.
21. Sode O, Hirata S. J. Phys. Chem. A. 2010; 114:8873. [PubMed: 20593764]
22. Jacobson LD, Herbert JM. J. Chem. Phys. 2011; 134 094118.
23. Nadig G, Van Zant LC, Dixon SL, Merz KM Jr. J. Am. Chem. Soc. 1998; 120:5593.
24. Van der Vaart A, Merz KM Jr. J. Am. Chem. Soc. 1999; 121:9182.
25. van der Vaart A, Merz KM Jr. J. Chem. Phys. 2002; 116:7380.
26. Wang B, Brothers EN, Van der Vaart A, Merz KM Jr. J. Chem. Phys. 2004; 120:11392. [PubMed: 15268173]
27. Gao J, Garcia-Viloca M, Poulsen TD, Mo Y. Adv. Phys. Org. Chem. 2003; 38:161.
28. Mo Y, Gao J. J. Phys. Chem. B. 2006; 110:2976. [PubMed: 16494296]
29. Mo Y, Song L, Lin Y. J. Phys. Chem. A. 2007; 111:8291. [PubMed: 17655207]
30. Mo YR, Bao P, Gao JL. Phys Chem Chem Phys. 2011; 13:6760. [PubMed: 21369567]
31. Isegawa M, Gao J, Truhlar DG. J. Chem. Phys. 2011; 135 084107.
32. Khaliullin RZ, Bell AT, Head-Gordon M. J. Chem. Phys. 2008; 128 184112.
33. Lee T-S, York DM, Yang W. J. Chem. Phys. 1996; 105:2744.
34. York DM, Lee T-S, Yang W. J. Am. Chem. Soc. 1996; 118:10940.
35. York DM, Lee T-S, Yang W. Phys. Rev. Lett. 1998; 80:5011.
36. Wada M, Sakurai M. J. Comput. Chem. 2005; 26:160. [PubMed: 15586398]
37. Xie W, Song L, Truhlar DG, Gao J. J. Phys. Chem. B. 2008; 112:14124. [PubMed: 18937511]
38. Song L, Han J, Lin YL, Xie W, Gao J. J. Phys. Chem. A. 2009; 113:11656. [PubMed: 19618944]
39. Wierzchowski SJ, Kofke DA, Gao J. J. Chem. Phys. 2003; 119:7365.
40. Xie W, Orozco M, Truhlar DG, Gao J. J. Chem. Theory Comput. 2009; 5:459. [PubMed: 20490369]
41. Sorakubo K, Yanai T, Nakayama K, Kamiya M, Nakano H, Hirao K. Theor. Chem. Acc. 2003; 110:328.
42. Cembran A, Song L, Mo Y, Gao J. J. Chem. Theory Comput. 2009; 5:2702. [PubMed: 20228960]
43. Gao J, Xia X. Science. 1992; 258:631. [PubMed: 1411573]
44. Gao, J. Rev. Comput. Chem. Lipkowitz, KB.; Boyd, DB., editors. Vol. Vol. 7. New York: VCH; 1995. p. 119
45. Gao J. J. Comput. Chem. 1997; 18:1062.
46. Svensson M, Humbel S, Morokuma K. J. Chem. Phys. 1996; 105:3654.
47. Frisch, MJ.; Trucks, GW.; Schlegel, HB.; Scuseria, GE.; Robb, MA.; Cheeseman, JR.; Scalmani, G.; Barone, V.; Mennucci, B.; Petersson, GA., et al. Gaussian 09. Rev. A.02 ed.. Wallingford, CT: Gaussian, Inc.; 2009.
48. Fedorov DG, Kitaura K. J. Chem. Phys. 2004; 121:2483. [PubMed: 15281845]
49. Fedorov DG, Kitaura K. Chem. Phys. Lett. 2004; 389:129.
50. Fedorov DG, Kitaura K. J. Chem. Phys. 2005; 123 134103/1.
51. Fedorov DG, Kitaura K. J. Chem. Phys. 2005; 122 054108/1.
52. Fedorov DG, Ishida T, Kitaura K. J. Phys. Chem. A. 2005; 109:2638. [PubMed: 16833570]
53. Mayhall NJ, Raghavachari K, Hratchian HP. J. Chem. Phys. 2010; 132
54. Hratchian HP, Krukau AV, Parandekar PV, Frisch MJ, Raghavachari K. J. Chem. Phys. 2011; 135
55. Gao J, Amara P, Alhambra C, Field MJ. J. Phys. Chem. A. 1998; 102:4714.
56. Amara P, Field MJ, Alhambra C, Gao J. Theor. Chem. Acc. 2000; 104:336.
57. Pu J, Gao J, Truhlar DG. J. Phys. Chem. A. 2004; 108:5454.
58. Pu J, Gao J, Truhlar DG. J. Phys. Chem. A. 2004; 108:632.
59. Pu J, Gao J, Truhlar DG. ChemPhysChem. 2005; 6:1853. [PubMed: 16086343]
60. Leverentz HR, Gao JL, Truhlar DG. Theor. Chem. Acc. 2011; 129:3.
61. Mo Y, Gao J, Peyerimhoff SD. J. Chem. Phys. 2000; 112:5530.
62. MacKerell AD Jr. J. Comput. Chem. 2004; 25:1584. [PubMed: 15264253]

63. Zhang P, Bao P, Gao JL. J. Comput. Chem. 2011; 32:2127.
64. Gao J, Wang Y. J. Chem. Phys. 2012; 136 080000.
65. Gianinetti E, Raimondi M, Tornaghi E. Int. J. Quantum Chem. 1996; 60:157.
66. Couty M, Bayse CA, Hall MB. Theor. Chem. Acc. 1997; 97:96.
67. Mo Y, Peyerimhoff SD. J. Chem. Phys. 1998; 109:1687.
68. Mo Y, Zhang Y, Gao J. J. Am. Chem. Soc. 1999; 121:5737.
69. Cembran A, Bao P, Wang Y, Song L, Truhlar DG, Gao J. J. Chem. Theory Comput. 2010; 6:2469. [PubMed: 20730021]
70. Jeziorski B, Moszynski R, Szalewicz K. Chem. Rev. (Washington, D. C.). 1994; 94:1887.
71. Stoll H, Preuss H. Theor. Chem. Acc. 1977; 46:12.
72. Xiang Y, Zhang DW, Zhang JZH. J. Comput. Chem. 2004; 25:1431. [PubMed: 15224387]
73. Duan LL, Mei Y, Zhang DW, Zhang QG, Zhang JZH. J. Am. Chem. Soc. 2010; 132:11159. [PubMed: 20698682]
74. Tong Y, Mei Y, Li YL, Ji CG, Zhang JZH. J. Am. Chem. Soc. 2010; 132:5137. [PubMed: 20302307]
75. Gao J, Cembran A, Mo Y. J. Chem. Theory Comput. 2010; 6:2402.
76. Salter EA, Trucks GW, Fitzgerald G, Bartlett RJ. Chem. Phys. Lett. 1987; 141:61.
77. Trucks GW, Salter EA, Sosa C, Bartlett RJ. Chem. Phys. Lett. 1988; 147:359.
78. Wiberg KB, Hadad CM, Lepage TJ, Breneman CM, Frisch MJ. J. Phys. Chem. 1992; 96:671.
79. Handy NC, Schaefer HF. J. Chem. Phys. 1984; 81:5031.
80. Mulliken RS. J. Chem. Phys. 1964; 61:20.
81. Xie W, Song L, Truhlar DG, Gao J. J. Chem. Phys. 2008; 128 234108/1.
82. Otto P, Ladik J. Chem. Phys. 1975; 8:192.
83. Fedorov DG, Ishida T, Uebayasi M, Kitaura K. J. Phys. Chem. 2007; 111:2722.
84. Stephens PJ, Devlin FJ, Chabalowski CF, Frisch MJ. J. Phys. Chem. 1994; 98:11623.
85. Zhao Y, Truhlar DG. Theor. Chem. Acc. 2008; 120:215.
86. Lynch BJ, Zhao Y, Truhlar DG. J. Phys. Chem. A. 2003; 107:1384.
87. Luo Y, Maeda S, Ohno K. J. Comput. Chem. 2009; 30:952. [PubMed: 18942728]

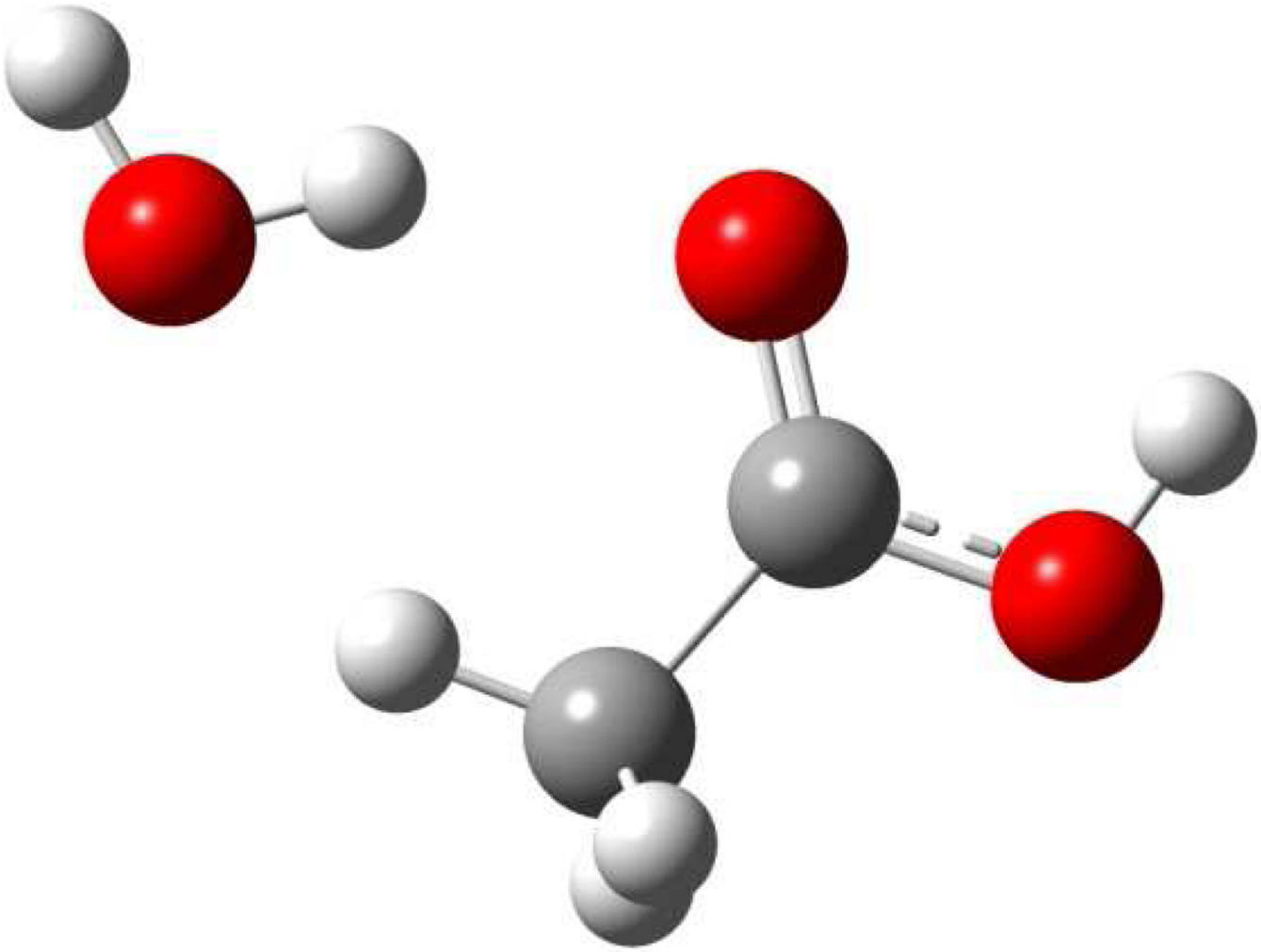

Figure 1.
Schematic illustration of the optimized configuration of acetic acid and water using M06/MG3S.

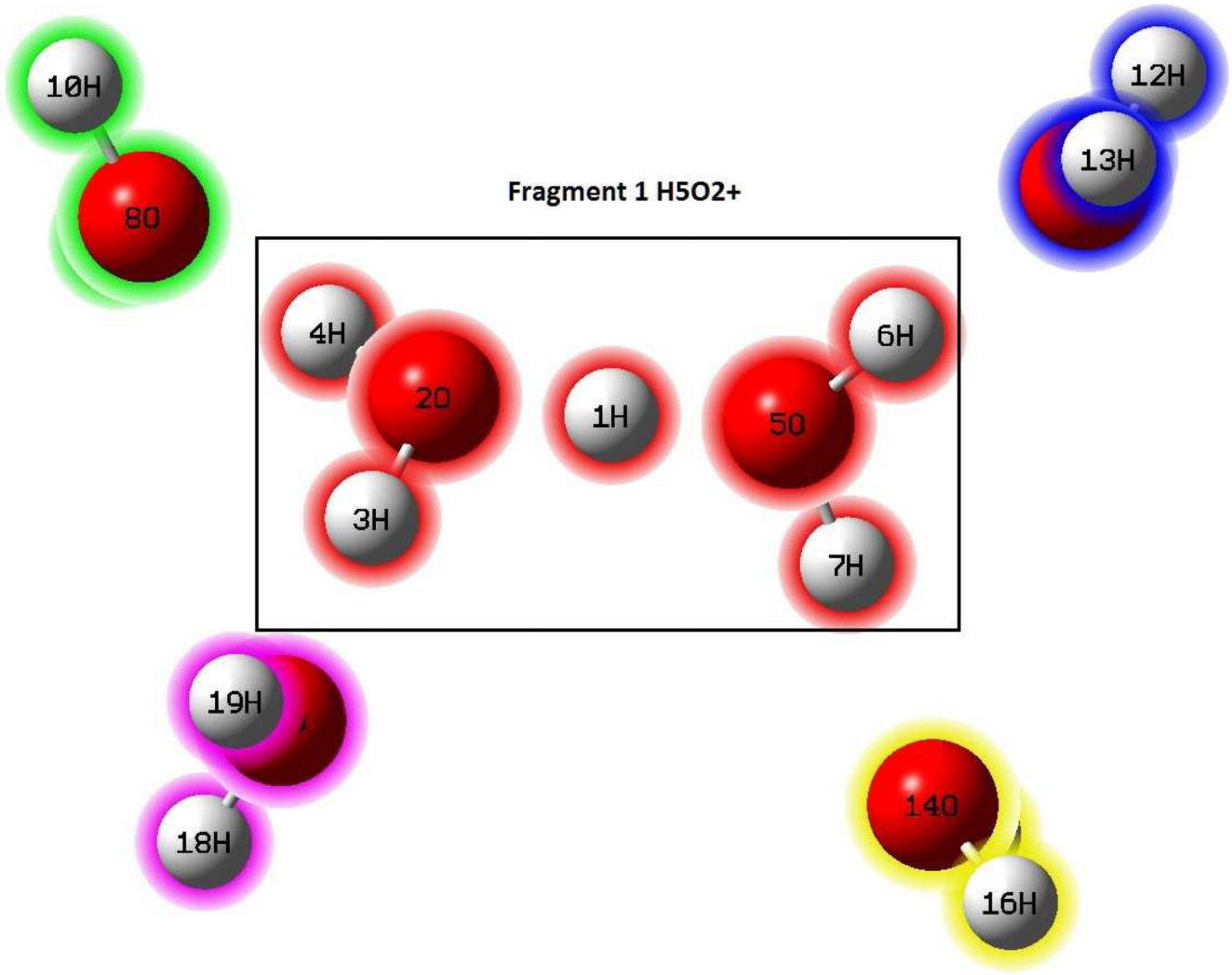

Figure 2.
Fragment partition of the $H_5O_2^+(H_2O)_4$ cluster optimized at the M06/MG3S.

Table 1

Computed binding energies and energy components (kcal/mol) between acetic acid (A) and water (B) using iterative charge-updating optimization in multilevel X-Pol. The 6-31G(d) basis set is used in all calculations at the M06/MG3S optimized geometries.

A	B	ΔE_{dist}	$\Delta E_A^{\mathrm{int}}(B)$	$\Delta E_B^{\mathrm{int}}(A)$	ΔE_{int}	ΔE_{b}[a]
X-Pol optimization by iteratively updating MK charges						
M06	M06	1.4	−9.1	−7.8	−8.4	−7.0
M06	B3LYP	1.4	−8.9	−7.6	−8.2	−6.8
M06	HF	1.6	−9.4	−8.2	−8.8	−7.2
MP2	HF	1.2	−8.8	−7.8	−8.3	−7.1
CCSD	M06	1.0	−8.7	−7.7	−8.2	−7.2
X-Pol optimization by iteratively updating MPA charges						
M06	M06	1.5	−9.6	−8.7	−9.2	−7.7
M06	B3LYP	1.5	−9.2	−8.5	−8.8	−7.3
M06	HF	1.8	−10.2	−9.2	−9.7	−7.9
MP2	HF	1.3	−9.5	−8.4	−9.0	−7.7
CCSD	M06	1.1	−9.1	−8.3	−8.7	−7.6
Full wave function calculation without fragmentation						
M06[b]						−6.9
CCSD(T)[b]						−6.6

[a] For the purposes of this table, the multilevel X-Pol calculations of ΔE_{b} are set equal to ΔE_{ele}, that is, they include the change in intramonomer energy and the electrostatic interaction energy but not the intermonomer exchange repulsion and dispersion terms

[b] Computed using the MG3S basis set at the M062X/MG3S geometries.

Table 2

Computed binding energies and energy components (kcal/mol) between acetic acid (A) and water (B) using the variational multilevel X-Pol. The 6-31G(d) basis set is used in all calculations at the M06/MG3S optimized geometries.

A	B	ΔE_{dist}	$\Delta E_A^{\mathrm{int}}(B)$	$\Delta E_B^{\mathrm{int}}(A)$	ΔE_{int}	ΔE_{ele}	ΔE_{XD}[a]	ΔE_{b}
X-Pol by variational optimization with MPA charges								
M06	M06	2.8	−10.1	−13.5	−11.8	−9.0	2.0	−7.0
M06	B3LYP	2.6	−9.7	−13.0	−11.3	−8.7	2.0	−6.7
M06	HF	3.1	−10.7	−14.2	−12.5	−9.4	2.0	−7.4
MP2	HF	4.3	−11.5	−13.1	−12.3	−8.0	2.0	−6.0
CCSD	M06	3.8	−11.0	−12.6	−11.8	−8.0	2.0	−6.0
Full wave function calculation without fragmentation								
M06[a]								−6.9
CCSD(T)[b]								−6.6

[a]The exchange-dispersion energy is estimated using the Buckingham terms with the parameters A_{OO} =1.5221×10^5 kcal/mol, B_{OO} = 3.754 Å^{-1}, and C_{OO} = 756.3 Å^6 kcal/mol for oxygen, and A_{CC} = 2.50178 ×10^6 kcal/mol, B_{CC} = 4.384 Å^{-1}, and C_{CC} = 1533.1 Å^6 kcal/mol for carbon.

[b]Computed at CCSD(T)/MG3S//M062X/MG3S.

Table 3

Computed binding energies and energy components (kcal/mol) between $H_5O_2^+$ and $(H_2O)_4$ using the iterative charge-updating optimization and variational multilevel X-Pol methods. The 6-31G(d) basis set is used in all calculations at the M06/MG3S optimized geometries.

$H_5O_2^+$	$(H_2O)_4$	ΔE_{dist}	ΔE_{int}	ΔE_{ele}	ΔE_{XD}	ΔE_b
X-Pol optimization by iteratively updating MK charges						
M06	M06	11.4	−100.5	−89.1	18.4	−70.7
M06	B3LYP	11.4	−99.0	−87.7	18.4	−69.3
M06	HF	11.3	−103.3	−92.0	18.4	−73.6
MP2	HF	10.9	−103.8	−92.9	18.4	−74.5
CCSD	M06	11.1	−100.6	−89.5	18.4	−71.1
X-Pol optimization by iteratively updating MPA charges						
M06	M06	11.5	−99.0	−87.5	18.4	−69.1
M06	B3LYP	11.4	−96.6	−85.2	18.4	−66.8
M06	HF	11.4	−103.1	−91.7	18.4	−73.3
MP2	HF	11.1	−103.7	−92.7	18.4	−74.3
CCSD	M06	11.2	−99.2	−88.0	18.4	−69.6
X-Pol by variational optimization with MPA charges						
M06	M06	10.7	−101.7	−91.0	18.4	−72.6
M06	B3LYP	11.3	−99.4	−88.1	18.4	−69.7
M06	HF	11.3	−105.8	−94.5	18.4	−76.1
MP2	HF	12.3	−106.7	−94.4	18.4	−76.0
CCSD	M06	18.5	−102.4	−83.9	18.4	−65.5
Full wave function calculation without fragmentation						
CCSD(T)[a]						−69.7

[a]Computed at CCSD(T)/MG3S//M062X/MG3S.